

Analysis and experimental validation of a sensor-based event-driven controller¹

J.H. Sandee

Eindhoven University of Technology, Dept. of Electr. Eng., Control Systems group

W.P.M.H. Heemels

Eindhoven University of Technology, Dept. of Mech. Eng., Control Systems Technology group

S.B.F. Hulsenboom

Océ Technologies BV, Venlo

P.P.J. van den Bosch²

Eindhoven University of Technology, Dept. of Electr. Eng., Control Systems group

Abstract: A challenging problem in the design of high-tech systems is servo control at high accuracy and at low cost price for its implementation. Conventional solutions are often not feasible, as high resolution encoders are far too expensive and high sample frequencies are prohibitive as controllers have to run on low-cost processors with processing power that is shared with many other tasks. As a possible solution, we present an event-driven controller that is based on an (extremely) low resolution encoder. The control value is updated at each moment that an encoder pulse is detected, yielding zero measurement error. However, as the time between two control updates is varying now, conventional controller design methods do not apply as they normally assume a constant sample time. To deal with this problem, the controller design is performed by transforming the system equations from the time domain to the position (spatial) domain, in which the encoder pulses, and therefore the controller triggering, are equidistant. In this way, the control problem is rewritten as a synchronous problem for a non-linear plant. A gain scheduled controller is designed and analyzed in the spatial domain. This event-driven controller is experimentally validated on a prototype printer in which a 1 pulse per revolution encoder is used to accurately control the motion of images through the printer. By means of analysis, simulation and experiments we show that the control performance is similar to the initially proposed industrial controller that has fixed (high) sample frequency and is based on a much higher encoder resolution. On top of this, the proposed event-driven controller involves a significant lower processor load.

1. Introduction

One of the challenging problems in the design of a printer, but also in many other high-tech systems, is the servo control of several motors at high accuracy. Conventional solutions are often too expensive as they rely on high resolution encoders. High sample frequencies are also prohibitive as controllers have to run on low-cost processors with processing power that is shared with many other tasks. Typical encoder resolutions are 500 pulses per revolution (PPR) with controllers running at 500 Hz. By using these high resolution encoders, measurement quantization errors can be neglected. However, to keep the system cost limited, our aim is to use a low resolution encoder to control a DC-motor. However, now the quantization errors become significant. To still achieve satisfactory control performance, this requires an adaptation of the conventional control algorithms.

Most applied and researched solutions that deal with low resolution sensor data use an observer-based approach to estimate the data at *synchronous* controller sample moments, based on *asynchronous* measurement moments [3,4,7,8,9]. In these solutions, the continuous-time plant is translated into a discrete-time model which is time-varying, as it depends on the time between successive measurement instants. The approaches in [4,7] use Kalman filtering. In [8], a Luenberger-type observer is applied to use asynchronous measurement data in combination with a multi-rate controller scheme. In tracking applications, a well-known technique is the $\alpha\beta$ -tracker [3] to estimate position, velocity and acceleration in a time-discrete manner. An overview of these

¹ This work is part of the Ph.D. thesis [1] and has been carried out as part of the Boderc project under the responsibility of the Embedded Systems Institute. This project is partially supported by the Dutch Ministry of Economic Affairs under the Senter TS program.

² Corresponding author: Tel: 040 2473760 / 040 2472300 Fax: 040 2434582 E-mail: p.p.j.v.d.bosch@tue.nl

methods and a comparison between them is presented in [9] in the application of using optical incremental encoders to measure position and velocity. The main drawback of these methods is that they generally require a high computational effort for computing the observer estimates.

In this paper we will use a different control paradigm that is simple to implement and does not suffer from the added complexity of an observer. The control structure is an asynchronous control scheme in which the control updates are triggered by the position measurement (encoder pulse). The idea of the asynchronous controller is based upon the observation that the position is *exactly* known at an encoder pulse and thus there is no need for an observer. However, as the velocity of the motor varies over time, both measurement and control updates are not equidistant in time. This requires a completely new design strategy for these event-driven controllers of which initial proposals were made in [6].

2. Problem description

We consider the control of a DC-motor that can be described by the second-order model

$$\begin{aligned}\dot{\theta}(t) &= \omega(t) \\ \dot{\omega}(t) &= \frac{1}{J} \left[\left(\frac{-k^2}{R} - B \right) \omega(t) + \frac{k}{R} u(t) - d(t) \right]\end{aligned}\quad (1)$$

where $\theta(t)$ [rad] is the angular position of the motor axis, $\omega(t)$ is its angular velocity [rad/s], $u(t)$ the motor voltage [V] and $d(t)$ the disturbance torque [Nm] at time t . The motor parameters are obtained from data sheets of the motor manufacturer: the motor inertia $J_m = 0.83 \cdot 10^{-4}$ kgm², the motor torque constant $k = 0.028$ Nm/A, the motor resistance $R = 1.0$ Ω and the motor damping $B = 3.0 \cdot 10^{-5}$ Nms/rad. The inertia of the load $J_l = 1.0 \cdot 10^{-4}$ kgm² is added to the motor inertia to obtain the total inertia J .

The industrial requirements for throughput and printing accuracy in the printer result in a feedback and feed-forward controller combination such that:

- The deviation from the steady-state position error is at most 0.25 rad during printing. Only deviations from a constant position error are visible in the print quality.
- All relevant disturbances are rejected sufficiently.

3. Event-driven control

For the event-driven controller we propose to execute both the measurement and the control update at the moment of a encoder pulse. The control updates are not equidistant in the time domain in this setting, which hampers the use of classical time-driven control schemes. However, we can apply variations of classical design methods, if we define the models of the plant and the controller in the spatial (angular position) domain instead of the time domain, as initially proposed in [6]. This idea is based on the observation that the encoder pulses arrive equally spaced in the spatial domain, as the encoder pulses have an equidistant distribution along the axis of the motor. To use this reasoning, we first have to transform the motor model as given in equation (1) to an equivalent model in which the motor angular position is the independent variable. After that we will show how the controller design can be performed using classical control theory.

3.1 Transformation to spatial domain

The transformation ideas are explained in [6] by the authors, which states:

$$\frac{d\theta}{dt}(t) = \omega(t) \Rightarrow \frac{dt}{d\theta}(\theta) = \frac{1}{\omega(\theta)} \quad (2)$$

where $\omega(\theta)$ denotes the angular velocity of the motor and $t(\theta)$ denotes the time, respectively, at which the motor reaches position θ . Under the assumption that $\omega(t) \neq 0$ (the motor does not change direction) for all $t > 0$, a one-to-one correspondence between θ and t exists and an interchange of their roles is possible.

Using (2) we obtain the motor model in the spatial domain:

$$\begin{aligned}\frac{dt}{d\theta}(\theta) &= \frac{1}{\omega(\theta)} \\ \frac{d\omega}{d\theta}(\theta) &= \frac{1}{J} \left[-\frac{d(\theta)}{\omega(\theta)} - \left(\frac{k^2}{R} + B \right) + \frac{k}{R} \cdot \frac{u(\theta)}{\omega(\theta)} \right] \\ y(\theta) &= t(\theta)\end{aligned}\quad (3)$$

where $d(\theta)$ and $u(\theta)$ denote the disturbance torque and the motor voltage, respectively, at motor position θ . Note that time t is now a function of θ and becomes a state variable in this new description. To consider the disturbance d as a function of the angular position θ is an advantage for many controller designs, as disturbance is often coupled to the angular position, instead of time. Moreover, the output $y(\theta)$ is now the time $t(\theta)$ at which the motor reaches position θ .

The error that is input for the feedback controller is now selected to be the difference between the measured time of an encoder pulse ($t_m(\theta)$) and the time at which the encoder pulse ideally should have occurred based on the reference trajectory (which is denoted by $t_r(\theta)$):

$$e_t(\theta) = t_r(\theta) - t_m(\theta) \quad (4)$$

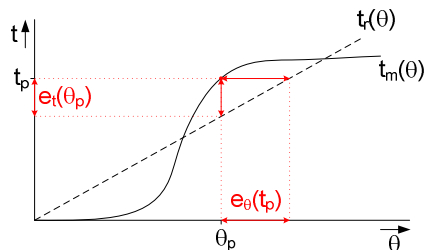


Figure 1: Errors in t and θ

In figure 1 it is shown how the *time error* can be translated into a *position error*. When ω_r is constant and non-zero in the time interval $(t_r(\theta_p), t_m(\theta_p))$ when $t_m(\theta_p) > t_r(\theta_p)$, or $(t_m(\theta_p), t_r(\theta_p))$ when $t_m(\theta_p) < t_r(\theta_p)$, where θ_p is the angular position at an encoder pulse detection, then it holds that

$$e_\theta(t_p) = -\omega_r e_t(\theta_p) \quad (5)$$

When ω_r is not constant, equation (5) can be used as an approximation with $\omega_r(\theta_p)$ or $\omega_r(t_p)$.

To satisfy the control objective that disturbances are sufficiently rejected, we consider the frequency content of these disturbances in the spatial domain: the *spatial frequency* [rad^{-1}]. The spatial frequency is a characteristic of any structure that is periodic across position in space. It is a measure of how often the structure repeats per unit of distance (completely analogous to 'ordinary' frequency with respect to time). The concept of spatial frequency is especially used in wave mechanics and image processing [5]. For many periodic movements the spatial frequency content is almost constant, while the regular frequency (in Hz) changes with changing speeds. For the disturbances in the example the main component is located at a spatial frequency of $8.0 \cdot 10^{-3} \text{ rad}^{-1}$. Originally, for time-driven control, this value was used in combination with the maximum velocity of the motor, to quantify the bandwidth with respect to time - in Hz. This clearly leads to non-optimal designs, when the motor also runs at lower velocities.

3.2 Controller design

The resulting model (3) is non-linear. It can be linearized around steady-state trajectories. The steady-state trajectory is chosen straightforwardly at a constant angular velocity ω_e of the motor after start-up:

$$(t_e, \omega_e, d_e, u_e) = \left(\frac{1}{\omega_e} \theta, \omega_e, d_e, k\omega_e + \frac{(B\omega_e + d_e)R}{k} \right) \quad (6)$$

where d_e is chosen as the mean value of the disturbance d . The variations around this steady-state trajectory are denoted by $(\Delta t, \Delta\omega, \Delta d, \Delta u)$. Hence, $t = t_e + \Delta t$, $\omega = \omega_e + \Delta\omega$, etc. The linearized dynamics are

$$\begin{aligned} \frac{d\Delta t}{d\theta}(\theta) &= -\frac{1}{\omega_e^2} \Delta\omega(\theta) \\ \frac{d\Delta\omega}{d\theta}(\theta) &= \frac{1}{J\omega_e} \left[-\left(\frac{k^2}{R} + B \right) \Delta\omega(\theta) - \Delta d(\theta) + \frac{k}{R} \cdot \Delta u(\theta) \right] \\ \Delta y(\theta) &= \Delta t(\theta) \end{aligned} \quad (7)$$

We can now design a feedback PD controller that compensates for the first-order variations $\Delta u(\theta)$ as defined in (7). The control value applied to the plant should be $u = u_e + \Delta u$. As $u_e = k\omega_e + \frac{B\omega_e R}{k} + \frac{d_e R}{k}$, the feed-forward term

takes care of $\left(k + \frac{BR}{k}\right)\omega_e$ and d_e has to be compensated for by the PD controller. Using the model parameters from section 2, we can compute the feed-forward $u_e = K_{ff}\omega_e$: $K_{ff} = k + \frac{BR}{k} = 0.029$.

We have chosen to design a PD controller and tuned it in the discrete *position* domain. We aim at using a minimal encoder resolution of only 1 PPR. Choosing this ultimately low resolution has the advantage that we do not have to deal anymore with inaccurate sensor distributions along the motor axis. To tune the controller, equation (7) was first discretized in the spatial domain, using a sample *distance* of 2π rad.

The PD controller was chosen as
$$H_{c1}(\hat{z}) = \frac{(K_p + K_d)\hat{z} - K_d}{\hat{z}}, \quad (8)$$

where the notation \hat{z} is used instead of z to emphasize that the discretization has been made in the spatial domain, instead of the time domain. Furthermore, this event-driven controller takes the time error as input. To find the values for the controller parameters K_p and K_d , we used the root-locus design method. For $\omega_e = 200, 300, 400$ and 500 rad/s and choosing $K_p = 1.0$ and $K_d = 12$ we obtain the root-locus as depicted in figure 2. The '+' marks indicate the roots for feedback gain 1. The root-locus shows different roots for the different speeds. For $\omega_e = 200$ rad/s the root-locus even indicates unstable behavior. Therefore, controller (9) is suggested, for which the root-locus is plotted in figure 3.

$$H_{c2}(\hat{z}) = \omega_e^2 \frac{(K_p + K_d\omega_e)\hat{z} - K_d\omega_e}{\hat{z}} \quad (9)$$

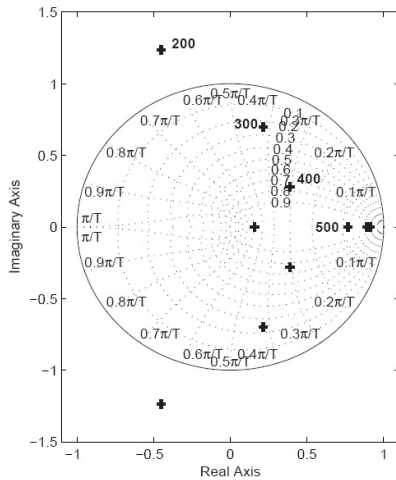


Figure 2: Root-locus for controller (8)

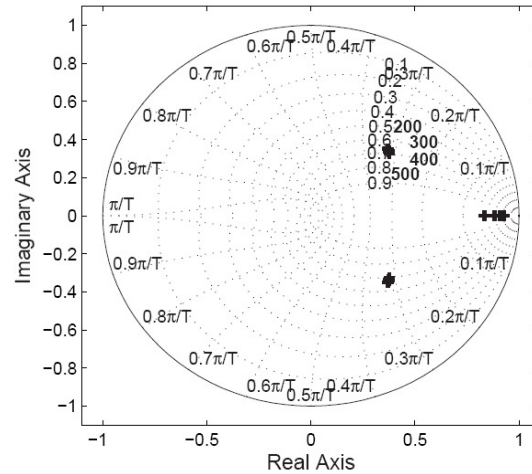


Figure 3: Root-locus for controller (9)

We computed the sensitivity function (for the linearized, discretized plant) as the transfer function from the disturbance $\Delta d(\theta)$ to $\Delta u_d(\theta)$. Both signals are indicated in figure 4, which shows a graphical representation of equation (7) together with feedback controller (9) for $\omega_e = 388$ rad/s. For the other evaluated velocities the plot looks similar. Note that \hat{s} is used instead of s to emphasize that the integration is performed in the spatial domain. The Bode magnitude plot of this discrete-position transfer is depicted in figure 5. Spatial frequencies up to the 0.01 rad^{-1} are attenuated. This satisfies the required bandwidth as given in section 3.1, being $8.0 \cdot 10^{-3} \text{ rad}^{-1}$.

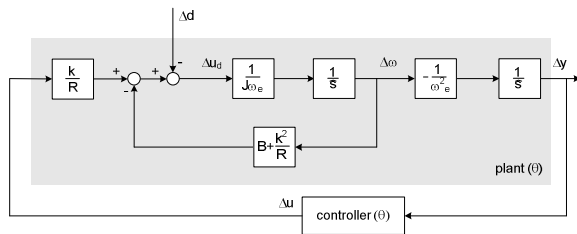


Figure 4: Graphical representation of linearized continuous dynamics (7)

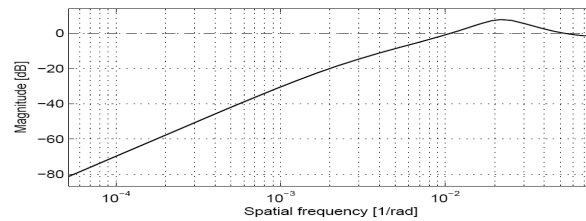


Figure 5: Bode mag. plot of transfer from $\Delta d(\theta)$ to $\Delta u_d(\theta)$ for $\omega_e = 388$ rad/s.

4. Experimental results

Experiments have been carried out on a complete prototype document printing system at Océ Technologies BV for both the originally implemented observer-based controller and the event-driven controller, in which a constant reference velocity of 388 rad/s is tracked. The observer-based controller operates with an encoder having a resolution of 12 PPR and at a sample frequency of 250 Hz [1]. The experimental results for both controllers are given in figures 6 and 7. These figures show the position error during printing over 5 seconds (after start-up). In this period, 5 sheets are printed at a speed of 80 pages per minute.

Comparing the results in figures 6 and 7 we observe similar control performance for the observer-based controller and the event-driven controller, both within spec. The maximum deviation from the average position error is for both controllers about 0.15 rad, which is smaller than 0.25 rad as required. However, the event-driven controller operates with an encoder with a resolution that is a factor 12 lower than that for the observer-based controller. Furthermore, the observer-based controller runs at a (constant) control sample frequency of 250 Hz and the event-driven controller at a much lower *average* frequency (approximately 62 Hz). The errors caused by the sheet passings can be distinguished in both figures, although there are more disturbances (at different frequencies) acting on the system as can be seen from the measurement data.

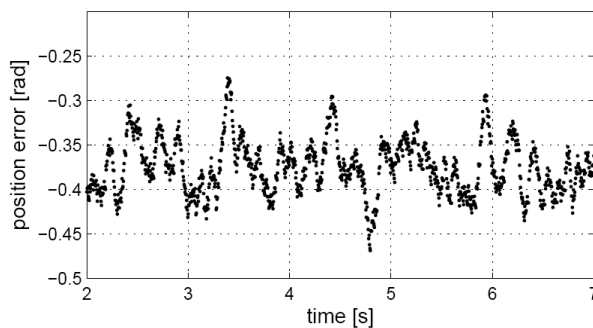


Figure 6: Experiment observer-based controller with 12 PPR encoder and sample freq. 250 Hz.

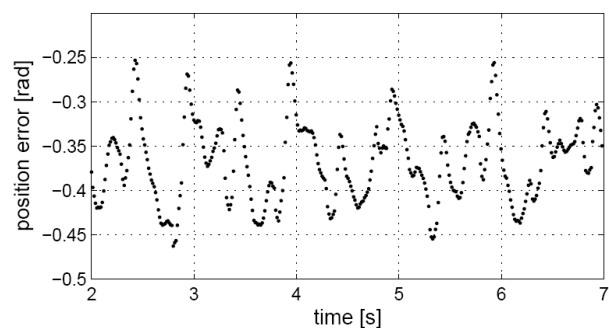


Figure 7: Experiment event-driven controller with 1 PPR encoder.

5. Conclusions

In this paper we presented the use of event-driven control to accurately control a DC-motor on the basis of an encoder having a resolution of 1 PPR. By means of analysis and industrial experiments we showed that the performance of the controller satisfied the requirements. Furthermore, we showed that similar control performance could be achieved compared to the initially proposed industrial observer-based controller. The advantages of the event-driven controller over the observer-based controller can be summarized as follows:

- Only a cheap encoder with a resolution of 1 PPR necessary, instead of 12 PPR
- Lower computational load for the processor (factor 5 reduction)
- Lower complexity of control algorithm (number of tuning parameters 2 instead of 4)

Experiments on a prototype printer validate the results and are very promising. Further research is still needed to fully comprehend such event-driven controllers and give systematic synthesis methods.

References

1. Sandee, J.H. (2006). Event-driven control in theory and practice, trade-offs in software and control performance. Ph.D. thesis, TU Eindhoven, ISBN: 90-386-1933-2.
2. Årzén, Karl-Erik (1999). A simple event-based PID controller. In: Proceedings of the 14th World Congress of IFAC. Beijing, P.R. China, vol. 18, pp. 423–428.
3. Friedland, B. (1973). Optimum steady-state position and velocity estimation using sampled position data. In: IEEE transactions on Aerospace and Electronic Systems. vol. AES-9, no. 6, pp. 906–911.
4. Glad, T. and L. Ljung (1984). Velocity estimation from irregular, noisy position measurements. In: Proceedings of the IFAC 9th Triennial World Congress, Budapest, no. 2, pp. 1069–1073.
5. Goodman, J. (2005). Introduction to fourier optics. 3rd ed., Roberts & Company, 2005.
6. Heemels, W.P.M.H., R.J.A. Gorter, A. van Zijl, P.P.J. van den Bosch, S. Weiland, W. Hendrix and M. Vonder (1999). Asynchronous measurement and control: a case study on motor synchronization. In: Control Engineering Practice, vol. 7, pp. 1467–1482.
7. Krucinski, M., Cloet, C., Tomizuka, M. and R. Horowitz (1998). Asynchronous observer for a copier paper path. In: Proceedings of the 37th IEEE Conference on Decision and Control, vol. 3, 1998, pp. 2611–12.
8. Phillips, A.M., and M. Tomizuka, (1995). Multirate estimation and control under time-varying data sampling with applications to information storage devices. In: Proc. American control conf., vol. 6, pp. 4151–4155.
9. Vottis, C.V. (2003), Extracting more accurate position and velocity information from optical incremental encoders, SAI/2yr thesis, Technische Universiteit Eindhoven, ISBN 90-444-0335-4.